

# Multiwavelength recording with a random pattern reference scheme

Ai Inoue,<sup>1</sup> Yoshihisa Takayama,<sup>2</sup> and Kashiko Kodate<sup>1,\*</sup>

<sup>1</sup>Faculty of Science, Japan Women's University, 2-8-1 Mejirodai, Bunkyo-ku, Tokyo 112-8681, Japan

<sup>2</sup>National Institute of Information and Communications Technology, 4-2-1 Nukuikita, Koganei-shi, Tokyo 184-8795, Japan

\*Corresponding author: [kkodate@fc.jwu.ac.jp](mailto:kkodate@fc.jwu.ac.jp)

Received 18 November 2009; revised 15 March 2010; accepted 15 March 2010;  
posted 15 March 2010 (Doc. ID 120070); published 20 April 2010

In a random-reference multiplexing scheme, we propose a method of generating different wavefronts without rotating a random pattern-generating element, simply by changing the wavelength of the incident light. A reference pattern with a random wavefront is an important aspect of color recording and readout. The color recording and readout system we propose is simple and compact, and generation of uncorrelated color patterns is easy. An important feature is that simultaneous readout using multiple wavelengths is facilitated. We confirmed the feasibility of this system by simulation and experiment, and we examined color recording and readout using multiple wavelengths. © 2010 Optical Society of America

*OCIS codes:* 210.2860, 090.4220.

## 1. Introduction

With the rapid development of information technology expected in the future, the amount of information prevalent in society will increase at an accelerated rate. In handling this information, security and confidentiality are extremely important. Holographic optical memories are able to enhance security by code hologram information in three dimensions.

Our research team proposed a random-reference multiplexing scheme that uses a holographic optical memory with a coded wavefront as a reference beam [1,2]. A reference pattern with a random wavefront is an important aspect for recording and readout. The generated patterns differ depending on the incident wavelength and the rotary angle and position of the reference pattern-generating element. The right image can be read out as long as the same reference pattern as was used in the recording process is input to the recording medium. However, the recorded information disappears gradually from the medium,

due to the characteristics of the photorefractive effect while the crystal is illuminated with light. Therefore, we consider this system suitable for secure applications.

In this system, a random wavefront can be generated by simply illuminating the random pattern-generating element. A compact system exhibiting the following two features can be easily achieved: first, multiplexing is possible by rotating the pattern-generating element. Second, precise optical axis control is not necessary because of the diffused light [3–8]. Our experiments confirmed the validity of our approach [2]. In order to enhance the security level, a fieldstone, serving as the random pattern-generating element, was proposed as a security key, and the performance was examined in some applications. One of the features of a fieldstone is that it is extremely difficult to reproduce the same optical characteristics, unlike artifacts. In addition, by processing fieldstones into fashion accessories, the degree of security can be improved because such fieldstone accessories are unlikely to be recognized as a key [9–12].

In this article, we propose a simple and compact color recording and readout system based on wave-

length-multiplexed recording, and we introduce a method for generating a different wavefront as a random pattern by changing the incident wavelength. We confirmed the feasibility of the system by simulation and experiment. First, we used only two wavelengths emitted by red and green lasers. Subsequently, we also examined color recording and readout using multiple wavelengths.

## 2. Principle of Color Recording and Readout

To confirm the feasibility of the random-reference multiplexing scheme, we constructed a Mach-Zehnder interferometer using a Nd:YVO<sub>4</sub> laser of wavelength  $\lambda_G = 532$  nm as a light source for hologram recording. The recording medium was a 45° cut LiNbO<sub>3</sub>:Fe photorefractive crystal with the dimensions 1 cm × 1 cm × 1 cm. A random pattern-generating element was placed in the optical path of the reference beam, whereas a spatial light modulator (SLM) or mask was placed in the object beam. The reference beam with a random phase distribution was set to interfere with the object beam carrying the image information to be recorded. The optical axis of the object beam was set perpendicular to that of the reference beam in order to mitigate the effects of scattered light emitted from the random pattern-generating element in the background of the readout image. The *c* axis was in the plane containing the object beam and the reference beam. Because the angle between the object beam and the reference beam was almost 90°, only the polarization components orthogonal to the plane interfered. Therefore, the polarizations of those beams were aligned with the ordinary polarization direction of the crystal. When irradiating the LiNbO<sub>3</sub> crystal with the reference beam, the readout images were acquired by a CCD camera connected to a PC. Multiplexed recording was carried out by rotating the random pattern-generating element.

Figure 1 illustrates the proposed method of generating different wavefronts by changing only the wavelength of the incident light. Figure 2 shows the experimental optical setup.

A simple and compact system is required to produce uncorrelated color patterns in a color recording and readout system functioning as a holographic op-

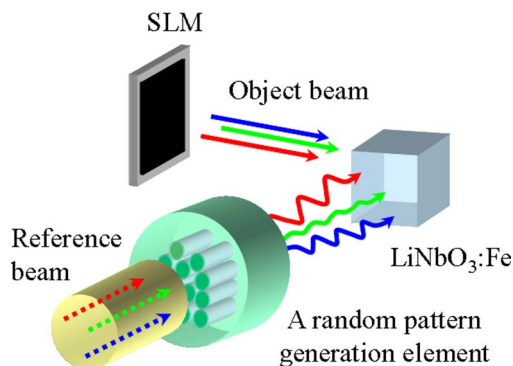


Fig. 1. (Color online) Principle of color recording.

tical memory using a photorefractive crystal [13,14]. For example, when generating a random pattern with a liquid crystal panel, the pattern obtained by transmitting light through the liquid crystal depends on the wavelength. However, for a given change in wavelength, the difference between the generated patterns may be small, i.e., a large correlation. On the other hand, in the method we propose, a completely different pattern is generated when the wavelength is changed, i.e., a small correlation. We used different wavelengths to estimate the difference between the generated patterns formed by a liquid crystal. For this estimation, we focused on the correlation between the generated patterns. The refractive index of the liquid crystal depends on wavelengths. For example, the refractive index for the wavelength G:550 nm is larger than the index for R:650 nm by about 0.01, given that the thickness of the liquid crystal cell is 5.0 μm [15]. We set up the random patterns of 128 × 128 pixels and generated the random patterns for the wavelengths G (pattern G) and R (pattern R). We computed the correlations between the two patterns, G and R, by changing the random patterns 10 times, and we found the averaged correlation coefficient is 0.36. In addition, we calculated the diffraction efficiencies. We defined the diffraction efficiency as the ratio of the intensity of the readout image to that of the recorded image. For this experiment, only pattern G was used as a reference beam for image recording. When the recorded hologram was read out by pattern G, the averaged diffraction efficiency was about 70.0%, while the efficiency when using pattern R was about 25.4%, which is regarded as cross talk. Therefore, when using a liquid crystal panel, it is essential to determine whether the correlation between the generated random patterns is sufficiently small to perform multiple hologram recording. Thus, simultaneous readout using multiple wavelengths is carried out, and for phase matching, we need to take into account the correlation of the random-reference patterns.

Because the pattern changes merely by changing the wavelength of the light incident on the random pattern-generating element, the color recording and readout system we propose is simple and compact, and the generation of uncorrelated color patterns is easy. Another important feature is that simultaneous readout using multiple wavelengths can be facilitated. Also, by combining the conventional method of rotating the random pattern-generating element with our new method involving changing the wavelength, the processing time can be reduced and the storage capacity can be increased.

## 3. Confirmation of the Operating Principle: Simulation

In order to confirm the operating principle of the wavelength-multiplexed color recording and readout, we examined readout images produced by simulation based on the photorefractive effect using MATLAB. It is helpful to estimate the recording conditions,

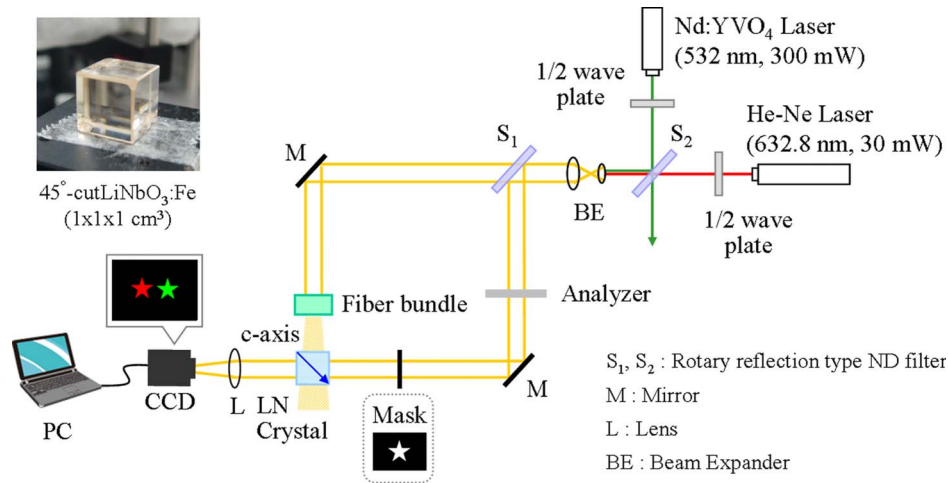


Fig. 2. (Color online) Optical setup of the color recording and readout system.

such as the optical power illuminating the crystal and the writing time, in order to reproduce the stored images with equivalent optical intensity. For convenience in the simulation, we assumed that the optical geometry for hologram recording is similar to codirectional two-wave mixing. Since we exploit the random-reference multiplexing scheme, the reference is provided as a randomly blurred wavefront that is changed in succession to record multiple holograms. In order to treat such a complex wave mixing process, we adopted a Fourier analysis approach in which the light illuminating the crystal is decomposed into a linear combination of plane waves. Although the transform has, in general, an integral form, we used an approximate expression given by a series expansion for convenience. Thus we can regard the holographic data storage as a two-wave mixing system containing  $N$  coherent waves, where each of these waves mutually interacts with the other  $N - 1$  waves. In this case, the interference pattern formed by these waves is described as

$$I = I_0 + \sum_j \sum_{l \neq j}^N A_j A_l^* \exp[i(\vec{k}_j - \vec{k}_l) \cdot \vec{r}] (\hat{e}_j \cdot \hat{e}_l) + c.c., \quad (1a)$$

$$I_0 = \sum_{j=1}^N |A_j|^2, \quad (1b)$$

where  $A_j$  is the amplitude of the  $j$ th component,  $\vec{k}_j$  is the wave vector,  $\hat{e}_j$  is the unit polarization vector,  $\vec{r}$  is the position vector, the asterisk denotes the complex conjugate, and *c.c.* denotes the complex conjugate of the preceding term. Since the process of hologram multiplexing requires more generalized equations for its description, we here take the influence of phase mismatching into consideration and derive a set of equations

$$\frac{\partial A_j}{\partial z} = \sum_{l=1}^N \sum_{m=1}^N Q_{jl} A_m \exp(i\Delta\vec{k}_{ml} \cdot \vec{z}), \quad (2a)$$

$$\tau \frac{\partial Q_{jl}}{\partial t} + Q_{jl} = \frac{\gamma_{jl}}{2I_0} A_j A_l^* (\hat{e}_j \cdot \hat{e}_l), \quad j \neq l, \quad (2b)$$

where  $\tau$  is the time constant,  $\gamma_{jl}$  is the coupling coefficient between  $j$ th and  $l$ th waves with  $\gamma_{jl} = \gamma_{lj}$ ,  $\Delta\vec{k}_{ml} = \vec{k}_m - \vec{k}_l$ . The coupling coefficient is a coefficient proportional to the refractive index change induced by the space electric field generated in the crystal. As a result, it is connected to the efficiency of two-wave mixing.  $Q$  represents the distribution of the index grating in the crystal. No hologram is recorded in the beginning, so the  $Q$  is set to 0 as initial value. As the hologram is being recorded,  $Q$  stores interference patterns formed by the object beam and the reference beam. When no external field is applied to the photorefractive material, the coupling coefficient can be regarded as a real number. Equation (2a) represents  $N$  equations, and Eq. (2b) includes  $N - 1$  equations. If we concentrate on the case  $l = m$ , the term  $\Delta\vec{k}_{ml}$  vanishes, and Eq. (2a) becomes identical to that in the previous work [16–19].

We performed a numerical simulation of the hologram multiplexing with the set of Eqs. (2a) and (2b). When we assume random-reference multiplexing, the random pattern newly generated before recording the  $n$ th image is temporarily illuminated after recording the  $(n - 1)$ th image.

First, in the color recording and readout system, the simulated readout images were examined at wavelengths of  $\lambda_R = 633$  nm,  $\lambda_G = 532$  nm, and  $\lambda_B = 403$  nm, which were used in the experiment described in the next section. Here, we assumed that holograms are recorded in the recording medium, that is, the LiNbO<sub>3</sub> crystal. The coupling coefficients,  $\gamma$ , for the respective wavelengths were calculated using a one-center model [20]. As a result of computation, we found that the ratio of the coupling coefficient for the wavelength  $\gamma_R$  to the coefficient for  $\gamma_G$  remains about 0.7 even if the propagation angle between the object beam and the reference beam is changed from 5° to 45°. Similarly, the ratio of the coupling coefficient for the wavelength  $\gamma_B$  to the one for  $\gamma_G$  is about 1.7. Thus, while regarding  $\gamma_G = 10$  cm<sup>-1</sup>, we assumed

$\gamma_R = 0.7 \text{ cm}^{-1}$ , and  $\gamma_B = 1.7 \text{ cm}^{-1}$ . Original images had  $32 \times 32$  pixels as the matrix, and the dimensions of the matrix for the reference beam were  $256 \times 256$ . It is assumed that the intensity of light illuminating the object is unity and the intensity of the reference is 10. We further introduced a normalization to define the time constant as 1 when the first image was recorded. We assumed a writing period of 0.1 for each image. Since the time constant is known to be inversely proportional to the total intensity illuminating the crystal [21], we modified the time constant at every writing period according to the image patterns. Figure 3(a) shows the results of computation using the same wavefront used in recording with the reference pattern as the readout. The readout images corresponding to wavelengths  $\lambda_R$ ,  $\lambda_G$ , and  $\lambda_B$  were calculated. Although the power ratios of the readout light were different for each wavelength, and the wavelength and  $\lambda_B$  was the most easy to record, the results indicate the possibility of using our approach for color recording and readout with wavelengths  $\lambda_R$ ,  $\lambda_G$ , and  $\lambda_B$ . The power ratios  $P$  of the readout light were  $P_R = 0.80$  and  $P_B = 2.00$ , with  $P_G$  set to 1.0.

Next, we examined the case of multiple wavelengths to confirm the possibility of simultaneous readout using multiple wavelengths with the same program. Here, we considered two wavelengths. The recording conditions were the same as in the presimulation described above for wavelength  $\lambda_R$ . Figure 3(b) shows the results of computation. We first recorded an image of the letter "R", followed by an image of the letter "G." Two images of the reference patterns used for recording each image were mixed. We assumed that the readout using this mixed image is identical to simultaneous readout using two wavelengths. As shown in Fig. 3(b), when the readout images corresponding to wavelengths  $\lambda_R$  and  $\lambda_G$  were calculated, the power ratios of the readout light were different for each wavelength, as in the previous calculation result. Nevertheless, simultaneous readout of both recorded images using two

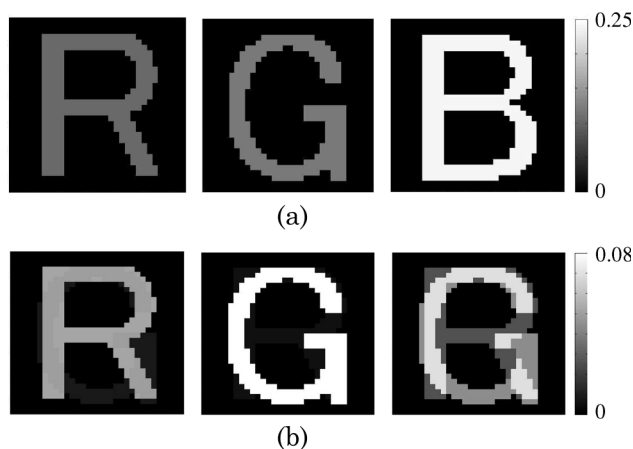


Fig. 3. Results from numerical simulation: (a) readout images using a single wavelength and (b) readout images using two-wavelength multiplexing. Left and center, single-wavelength  $\lambda_R$  or  $\lambda_G$ ; right, simultaneous readout using two wavelengths.

wavelengths as cross talk was confirmed. Therefore, the results of numerical simulation indicated the possibility of simultaneous readout using multiple wavelengths.

#### 4. Confirmation of the Operating Principle: Experiment

We then examined whether the operating principle could be confirmed by experiment using an He-Ne laser of wavelength  $\lambda_R = 632.8 \text{ nm}$  as a light source. Two light waves of wavelength  $\lambda_R$  interfered at the LiNbO<sub>3</sub> crystal, and the change in intensity between the two light waves due to diffraction by the grating formed in the crystal was measured. This result confirmed that it was possible to record and read out even with wavelength  $\lambda_R$ . In addition, we confirmed the ability to record and read out images even though one light wave became a random wavefront at one end of the fiber bundle.

Figure 4 shows the optical setup. An He-Ne laser was used as a light source, and a LiNbO<sub>3</sub> crystal was used as a recording medium for hologram recording. The angle between the two light waves was  $\theta = 10^\circ$ , and the angle between the  $c$  axis and the central axis of the two beams was set to  $45^\circ$  to cause interference using the extraordinary component. The ratios of the intensities of the two beams were 1:10 without the fiber bundle and 1:32 with the fiber bundle. The two light waves interfered at the LiNbO<sub>3</sub> crystal, and the change in intensity between the two light waves was measured with the two powermeters. Figures 5(a) and 5(b) show the results of the experiment with the ordinary beam. The change in intensity between the two light waves was confirmed with and without the fiber bundle. Therefore, the form of the hologram in the crystal was confirmed. The images in Fig. 5 are the readout beam and reference beam acquired by a CCD camera after measuring the powers. The readout light could still be obtained even if one of the two light waves was blocked. These results, together with the results of the multiple recording experiment using wavelength  $\lambda_G$ , demonstrate the feasibility of color recording and readout using multiple wavelengths.

In addition, we performed the same experiment with the extraordinary beam and compared the results with those described above. As a result of the

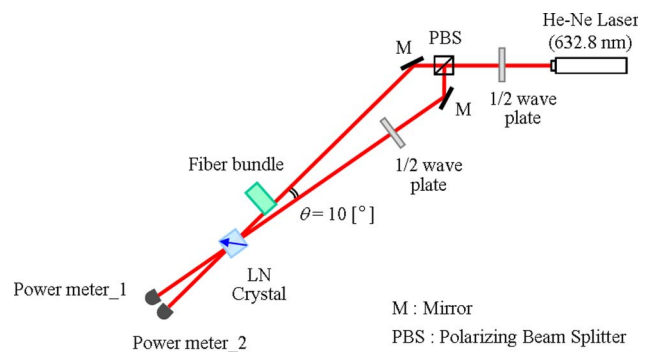


Fig. 4. (Color online) Optical setup to confirm the principle of the color recording and readout system by experiment.

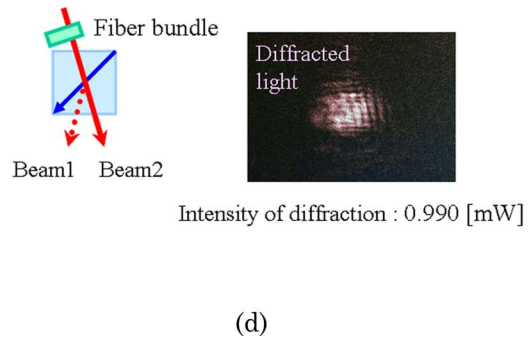
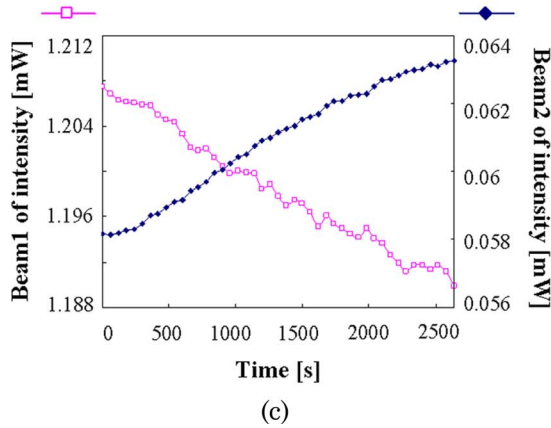
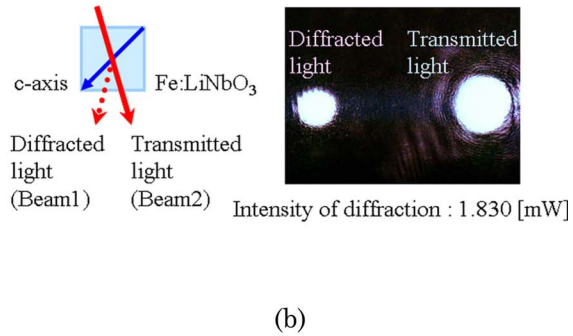
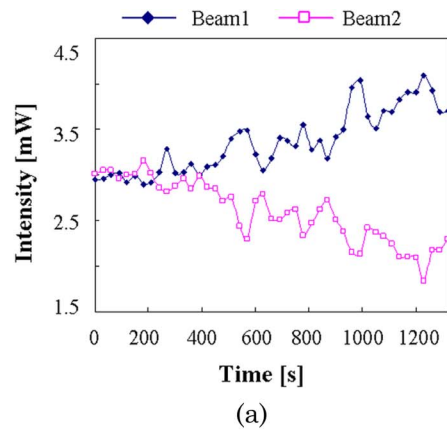


Fig. 5. (Color online) Experimental results from confirmation of operating principle: (a) and (b) are results without the fiber bundle. Images (c) and (d) are results with the fiber bundle. (a) and (c) The wave mixing characteristics when light waves illuminate the crystal. (b) and (d) Images of when only the light passing through the fiber bundle is turned on.

large change in intensity achieved using the ordinary beam, it was easier to record with the ordinary beam than with the extraordinary beam. Accordingly, we adopted an ordinary beam when constructing the optical setup of the color recording and readout system described below.

### 5. Color Recording and Readout Experiment

On the basis of the results in the sections above, we constructed the optical setup of the color recording and readout system with two wavelengths, shown in Fig. 2. In the setup shown in Fig. 2, so that the light intensity illuminating the crystal could be adjusted, we employed a rotary reflection-type ND filter  $S_1$  that combines the beams of wavelength  $\lambda_R$  and  $\lambda_G$  onto the same optical axis and another filter  $S_2$

that separates the single combined beam into two light waves for the Mach-Zehnder interferometer. It is assumed that the intensity illuminating an object is unity and the intensity of the reference is 10. The recording time was 10 min for wavelength  $\lambda_G$  and 120 min for wavelength  $\lambda_R$ . As the random pattern-generating element, a fiber bundle was placed in the reference beam. We examined the color recording and the readout using multiple wavelengths. Figure 6 shows the results of the experiment. After recording, we succeeded in obtaining each readout image as a result of a single incident wavelength  $\lambda_R$  or  $\lambda_G$ . Simultaneous readout using two wavelengths was also successful. Therefore, we experimentally confirmed the validity of our approach.

### 6. Conclusions

In this paper, we proposed a method for generating different wavefronts as random patterns simply by changing the wavelength of light incident on the random pattern-generating element, and we presented a color recording and readout system based on wavelength-multiplexed recording. This system is simple and compact, and the generation of uncorrelated color patterns is easy. Additionally, simultaneous readout using multiple wavelengths is straightforward. By combining the conventional method of rotating

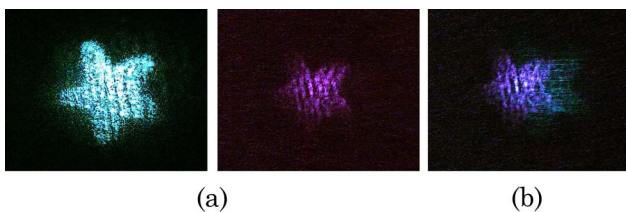


Fig. 6. (Color online) Readout images. (a) Single-wavelength: left, wavelength  $\lambda_G$ ; right, wavelength  $\lambda_R$ . (b) Simultaneous readout using two wavelengths.

the random pattern-generating element with our new method, the processing time of data readout can be reduced and the storage capacity can be increased.

First, in order to confirm the feasibility of the color recording and readout system with multiple wavelengths, we demonstrated the operating principle both numerically and experimentally. The numerical simulation indicated the possibility of color recording and readout with multiple wavelengths, and the experiment with an He–Ne laser source confirmed the two-wave mixing via the photorefractive effect. Next, on the basis of these results, we constructed an optical setup for the two-wavelength recording system. We examined the wavelength-multiplexed storage and successfully showed both a simultaneous readout and a separate readout.

For the future, we aim to improve data security by using a fieldstone as the random pattern-generating element and by optimizing the recording conditions. Additionally, we aim to combine the conventional method with the method proposed here to enhance the storage capacity and reduce the processing time for data readout.

## References

1. Y. Takayama, Y. Okazaki, J. Zhang, T. Aruga, and K. Kodate, "Method of hologram multiplexing by use of a fiber bundle with rotary movement," *Appl. Opt.* **43**, 1331–1336 (2004).
2. Y. Okazaki, Y. Takayama, E. Watanabe, and K. Kodate, "Animation recording system by rotating fiber bundle," *Rev. Laser Eng.* **33**, 399–403 (2005).
3. C. C. Sun, W. C. Su, B. Wang, and Y. O. Yang, "Diffraction selectivity of holograms with random phase encoding," *Opt. Commun.* **175**, 67–74 (2000).
4. Y. Jeong and B. Lee, "Effect of a random pattern through a multimode-fiber bundle on angular and spatial selectivity in volume holograms: experiments and theory," *Appl. Opt.* **41**, 4085–4091 (2002).
5. J. Zhang, S. Yoshikado, and T. Aruga, "Shift multiplexing for holographic storage system using fiber bundle referencing scheme," *Appl. Phys. Lett.* **82**, 25–27 (2003).
6. W. C. Su and C. H. Lin, "Enhancement of the angular selectivity in encrypted holographic memory," *Appl. Opt.* **43**, 2298–2304 (2004).
7. S. Han, Y. Jeong, J. Paek, T. Kim, and B. Lee, "Characteristics of remote hologram multiplexing with random pattern references from multimode fiber bundle," *Opt. Eng.* **43**, 2040–2047 (2004).
8. B. Lee, S. Han, Y. Jeong, and J. Paek, "Remote multiplexing of holograms with random patterns from multimode fiber bundles," *Opt. Lett.* **29**, 116–118 (2004).
9. Y. Ishii, Y. Takayama, M. Irisawa, E. Watanabe, and K. Kodate, "Random patterns optical multiple recording by rotating fieldstone and simulation of hologram multiplexing," in *Technical Digest of International Symposium on Optical Memory 2006* (Adthree Publishing, 2006), pp. 216–217.
10. Y. Ishii, Y. Takayama, A. Inoue, and K. Kodate, "A security key for wearing to record hologram with random-reference multiplexing scheme," in *Technical Digest of International Symposium on Optical Memory 2007* (ISOM, 2007), pp. 198–199.
11. Y. Ishii, Y. Takayama, and K. Kodate, "All-optical animation projection system with rotating fieldstone," *Opt. Exp.* **15**, 7218–7223 (2007).
12. A. Inoue, Y. Takayama, Y. Ishii, and K. Kodate, "Removeable fieldstone security key used in random pattern optical multiple recording," *Jpn. J. Appl. Phys.* **47**, 5960–5963 (2008).
13. Q. Sun, Y. Li, J. Xu, X. Zhang, G. Zhang, S. Liu, and G. Zhang, "Recognition of color patterns using a photorefractive LiNbO<sub>3</sub>:Fe crystal," *Opt. Commun.* **157**, 23–26 (1998).
14. C. A. Heid, B. P. Ketchel, G. L. Wood, R. J. Anderson, and G. J. Salamo, "3D, true color photorefractive hologram," in *Proceedings of the Materials, Fundamentals and Applications Topical Meeting, Nonlinear Optics '98* (IEEE, 1998), pp. 182–184.
15. Y. Ohno, T. Ishinabe, T. Miyashita, and T. Uchida, "Highly accurate method for measuring ordinary and extraordinary refractive indices of liquid crystal materials," IEICE technical report EID2007-82 (Institute of Electronics, Information and Communication Engineers, 2007).
16. M. Segev, Y. Ophir, and B. Fischer, "Nonlinear multi two-wave mixing, the fanning process and its bleaching in photorefractive media," *Opt. Commun.* **77**, 265–274 (1990).
17. M. Snowbell, M. Horowitz, and B. Fischer, "Dynamics of multiple two-wave mixing and fanning in photorefractive materials," *J. Opt. Soc. Am. B* **11**, 1972–1982 (1994).
18. T. Yoshida, A. Okamoto, Y. Takayama, and K. Sato, "Operable conditions of the beam-fanning novelty filter for the *c* axis and the incident angle," *Appl. Opt.* **39**, 5940–5948 (2000).
19. Y. Takayama, Y. Okazaki, T. Aruga, and K. Kodate, "A simple method for holographic recording of images in different polarization states using a fiber bundle with rotary movement," *Proc. SPIE* **5636**, 467–474 (2005).
20. M. C. Bashaw, T.-P. Ma, and R. C. Barker, "Comparison of single- and two-species models of electron–hole transport in photorefractive media," *J. Opt. Soc. Am. B* **9**, 1666–1672 (1992).
21. P. Yeh, *Introduction to Photorefractive Nonlinear Optics* (Wiley, 1993).